# Structure and Orientation of Pancreatic Colipase in a Lipid Environment: PM-IRRAS and Brewster Angle Microscopy Studies†

Maya Allouche,§ Sabine Castano,‡ Damien Colin,§ Bernard Desbat,‡ and Brigitte Kerfelec*,§

*INSERM, U476 "Nutrition Humaine et Lipides", Marseille, F-13385 France, INRA, UMR1260, Marseille, F-13385 France, Université Méditerranée Aix-Marseille 2, Faculté de Médecine, IPHM-IFR 125, Marseille, F-13385 France, and CBMN, UMR5248, CNRS, Université Bordeaux I, ENITAB, 2, rue Robert Escarpit, 33607 Pessac, France*

*Received September 7, 2007; Revised Manuscript Received October 12, 2007*

ABSTRACT: Colipase is a key element in lipase-catalyzed dietary lipids hydrolysis. Although devoid of enzymatic activity, colipase promotes pancreatic lipase activity in the physiological intestinal conditions by anchoring the enzyme on the surface of lipid droplets. Polarization modulation infrared reflection absorption spectroscopy combined with Brewster angle microscopy studies was performed on colipase alone and in various lipid environments to obtain a global view of both conformation and orientation and to assess lipid perturbations. We clearly show that colipase fully inserts into a dilaurin monolayer and promotes the formation of lipid/protein domains, whereas in a phospholipid environment its insertion is only partial, limited to the polar head group. In a mixed 70% phosphatidylcholine/30% dilaurin environment, colipase adsorbs to but does not penetrate deeply into the film. It triggers the formation of diglyceride domains under which it would form a rather uniform layer. We also clearly demonstrate that colipase adopts a preferred orientation when dilaurin is present at the interface. In contrast, at a neutral phospholipid interface, the infrared spectra suggest an isotropic orientation of colipase which could explain its incapacity to reverse the inhibitory effects of these lipids on the lipase activity.

Initiated in the stomach through the action of gastric lipase (*1*), the digestion of dietary triglycerides is completed in the duodenum through the combined action of pancreatic lipase (triacylglyceride ester hydrolase, EC 3.1.1.3), colipase, and bile secretion. In vivo, lipase substrates are presented as emulsified particles, the dietary fat droplets, stabilized by a monolayer surface rich in phospholipids, bile salts, and various proteins. Only 4 mole percent, at most, of long chain triglycerides are present at the surface of the droplet (*2*). This pool of interfacial substrate, which could be in dynamic equilibrium with the triglyceride core of the droplet, probably regulates the lipase activity (*3*). Except for the triglycerides, all the surface constituents are known to inhibit lipase activity in vitro (*4*−*7*) unless colipase is present, mainly by preventing lipase adsorption to the interface. Therefore, the primary role of colipase in triglyceride hydrolysis is to anchor the lipase to the water/lipid interface in the presence of physiological concentrations of biliary lipids.

Procolipase is a small protein made of 95 amino acids which has no enzymatic activity of its own. It is rapidly proteolyzed to a shorter form (colipase) by cleavage of the Arg5-Gly6 peptide bond (*8*). It is generally accepted that, at physiological pH, the conversion of procolipase to colipase has no functional consequence (*9*). Colipase is a small, amphipathic, and rather flat protein which lacks extensive secondary structure. It is made of a central region of two $\beta$-sheets held together by disulfide bonds, with four finger-shaped regions connected by type I $\beta$-turns protruding from this central region and an N-terminal region with no apparent secondary structure (no electron density in the X-ray structure) (*10*−*12*). Two short stretches of $\alpha$-helical residues are observed, one (residues 22−24) in the first finger (residues 14−23) and the other one in the last finger (residues 76−80). The tips of these loops, because of the predominance of hydrophobic residues, are thought to be devoted to lipid binding. In particular, the role of aromatic residues at the micelle−colipase interface has been emphasized (*13*−*15*). Colipase binds almost exclusively to the lipase C-terminal domain, its plane being rather perpendicular to the lipase $\beta$-sheet domain. However, in the structures of the active complex, colipase also interacts with the lipase lid (*11*, *12*). This interaction stabilizes the lipase lid in the open conformation, enlarges the hydrophobic patch presumably involved in the interaction of the lipase/colipase complex with the water/lipid interface, and thus facilitates lipase activity.

The effect of colipase on lipolysis has been extensively studied both by monolayer techniques (*16*, *17*) and emulsion of short and long chain triglycerides (*18*, *19*). However, whether colipase binds to the interface alone or as a complex with lipase is still not really elucidated. Some arguments suggest that lipase may form, in solution, an active complex with colipase and biliary lipid micelles, this complex representing the functional unit able to bind the emulsified oil droplets and to perform catalysis (*11*). For other authors, colipase binds first to the interface, inducing a lateral

† Maya Allouche's Ph.D. research was supported by a French-Tunisian grant from the French Ministry.

* Author to whom correspondence should be addressed. Tel: (33) 491 29 41 10. Fax: (33) 491 78 21 01. E-mail: Brigitte.Kerfelec@medecine.univ-mrs.fr.

§ INSERM, U476 "Nutrition Humaine et Lipides", INRA, UMR1260, and Université Méditerranée Aix-Marseille 2.

‡ Université Bordeaux I.

10.1021/bi701831f CCC: $37.00 
Published on Web 12/04/2007

redistribution of the lipids in the monolayer (*20*, *21*) which will favor the binding of lipase. As well, the mechanism by which colipase restores the activity of pancreatic lipase in the presence of biliary lipids remains unclear. In vitro, colipase is able to counteract lipase inhibition by bile salts but cannot reverse the inhibition by phospholipids unless bile salts are present. Moreover, the lipase activity is inhibited by ionic and non-ionic detergents irrespective of their charge and structure despite the presence of colipase (*4*, *22*). Full reversal of inhibition requires the presence of bile salts.

Finally, despite all these studies, the mechanism of action of colipase is still not fully understood. In particular, how colipase interacts with lipids, its orientation at the water/lipid interface, and the lipid perturbations induced by colipase adsorption remain intriguing questions.

As demonstrated in many studies (*23*−*26*), Langmuir monomolecular films provide a convenient model to study the properties of surface active proteins at the air/water interface and their adsorption process at a lipid interface. Obviously, the model in monolayer is appropriate to determine the molecular orientations only if the protein interacts with one half of a membrane in the natural state. Polarization modulation infrared reflection absorption spectroscopy (PM-IRRAS[1]) is a very useful technique to detect, in situ, proteins at an air/water interface or inserted in lipid monolayer and thus to determine their conformational structure and orientation. Indeed, the amide I (∼1650 $cm^{-1}$) and amide II (∼1550 $cm^{-1}$) bands of PM-IRRAS spectra are probes for proteins since the peptide amide bond is a basic functional group in proteins (*27*). The shape and position of these bands can be used to estimate the conformation and orientation of protein (*28*). The amide I band is the most sensitive one to evaluate the change in protein conformation and/or orientation at the water surface. The lipid perturbations induced by the adsorption of proteins can also be investigated through analysis of the lipid C═O stretching band (1730 $cm^{-1}$), the symmetric and antisymmetric $\nu(CH_2)$ groups (2920−2850 $cm^{-1}$), and eventually the polar head group vibrational mode (1230−990 $cm^{-1}$). The BAM is a powerful tool for observation of the evolution of a monolayer at the air/liquid interface. It allows visualization of the presence of phase-separated domains at water/lipid interface and thereby the effect of proteins on the domains formation.

In this paper, we study the adsorption of colipase at three different water/lipid interfaces: (1) a monolayer of dilaurin, a diglyceride used as a model lipase substrate; (2) a L-α-PC monolayer used as model of biliary lipids (the main components of the lipid droplet surface); (3) one monolayer of mixed 70% L-α-PC/30% dilaurin (mol/mol) to mimic the lipid droplet surface. We combine the two techniques to investigate, for the first time, the structure and the orientation of colipase at the water/lipid interface as well as the lipid-induced perturbation.

## MATERIALS AND METHODS

*Chemicals.* L-α-Phosphatidylcholine from egg yolk with fatty acid contents of approximately 33% 16:0 (palmitic), 13% 18:0 (stearic), 31% 18:1 (oleic), and 15% 18:2 (linoleic) (other fatty acids being minor contributors) and mixed isomers 1,2 and 1,3 dilaurin were from Sigma Aldrich. Lipids were purchased as powder and dissolved in chloroform ($CHCl_3$) from Carlo Erba. The concentration of the lipid solutions is 1 mg/mL.

*Colipase Purification.* Porcine pancreatic colipase was purified from a delipidated acetonic pancreatic powder as previously described (*29*). The protein concentration was determined at 280 nm using $E^{1\%} = 4.0$ (*30*). The isoelectric point is 5 (*29*). The enzyme solutions were freshly prepared at a concentration of 0.5 mg/mL for PM-IRRAS measurements and 2 mg/mL for BAM experiments.

*Film Formation and Surface Pressure Measurements*. Monolayer experiments were performed on a computer-controlled Langmuir film balance (Nima Technology, Coventry, England). The rectangular trough ($V = 60$ mL, $S = 105$ $cm^2$) and the barrier were made of Teflon. The surface pressure was measured by the Wilhelmy method using a filter paper plate. The trough was filled with a 10 mM Tris-HCl buffer pH 7.5, containing 0.1 M NaCl and 5 mM $CaCl_2$ using ultrapure water (Milli-Q, Millipore). The experiments were carried out at 25 ± 2 °C. The pure lipid monolayer was made by spreading the lipid at the air/water interface from chloroform solutions and then slowly compressing from 0 mN/m up to 18-20 mN/m. This target pressure corresponds to the pressure at which human lipase, the enzymatic partner of colipase, displays its higher activity on a dilaurin monolayer (personal data). For comparison, the same experiments were also performed at a target pressure of 30 mN/m which is the pressure observed in biological membranes. All the experiments were done at constant target pressure, and the area of the trough was simultaneously recorded during the injection of the colipase (33 or 40 nM) into the subphase.

*PM-IRRAS Spectroscopy.* PM-IRRAS spectra were recorded on a Nicolet Nexus 870 spectrometer equipped with a photovoltaic HgCdTe detector (SAT, Poitiers) cooled at 77 K. Generally, 300 or 600 scans were coadded at a resolution of 8 $cm^{-1}$ for colipase or mixed colipase/lipid monolayer, respectively. In short, PM-IRRAS combines FT-IR reflection spectroscopy with fast polarization modulation of the incident beam between parallel (p) and perpendicular (s) polarization. Two-channel processing of the detected signal makes it possible to obtain the differential reflectivity spectrum:

$$\Delta R/R = (R_p - R_s)/(R_p + R_s)J_2$$

To remove the contribution of liquid water adsorption and the dependence on Bessel functions $J_2$, the monolayer spectra are divided by that of the subphase. Under this condition, using an incidence angle of 75°, one selection rule appears; transition moments preferentially oriented in the plane of the interface give intense and upward oriented bands, while perpendicular moments give weaker and downward oriented bands.

*BAM Measurements.* The morphology of pure lipids or mixed protein/lipid monolayers at the air/water interface were observed using a Brewster angle microscope (NFT BAM*2plus*, Göttingen, Germany) mounted on the Langmuir trough. The microscope was equipped with a frequency doubled Nd:Yag laser (532 nm, 50 mW), polarizer, analyzer, and a CCD camera. The spatial resolution of the BAM was about 2 μm,

[1] Abbreviations: L-α-PC, L-α-phosphatidylcholine; PM-IRRAS, polarization modulation infrared reflection absorption spectroscopy; BAM, Brewster angle microscopy.

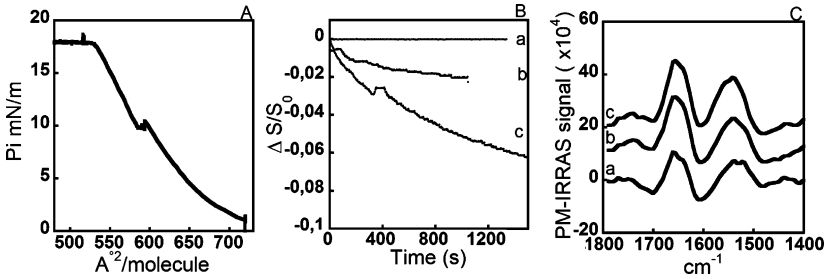


FIGURE 1: Adsorption of colipase at an air/buffer interface. (A) Surface pressure−area isotherm of porcine colipase. (B) Stability of the colipase film at different lateral pressures. (a) 1.1 mN/m, (b) 10 mN/m, and (c) 18 mN/m. (C) PM-IRRAS spectra of colipase (a) 1.1 mN/m, (b) 10 mN/m, and (c) 18 mN/m. Subphase: 10 mM Tris-HCl buffer containing 100 mM NaCl and 5 mM $CaCl_2$ pH 7.5. $[colipase]_{subphase}$ = 33 nM.

and the image size 600 × 450 $\mu$m with ×10 lens used. The BAM images are coded in gray level, which can be calibrated in absolute reflectance. The calibration function is established at each speed of the camera by comparison between the experimental curve of the gray level as a function of the incidence angle and the theoretical Fresnel curve on the water surface. The evaluation of the thickness was obtained using the software included in the BAM instrument. This software is based on the proportionality relation between the reflectance and the square of the interfacial film thickness when the optical index of the film is assumed constant. Moreover, BAM also gives some information on the fluidity of the film in relation with the geometry of the domains observed at the water surface.

## RESULTS

*Behavior of Colipase at the Air/Buffer Interface.* Upon injection of colipase (33 nM) in the subphase, the surface pressure slowly increased and reached a constant value of 1.1 mN/m after about 18 min. The mean apparent surface area of colipase was about 720 Å$^2$/molecule (Figure 1A), a slightly lower value than the various surface area (750, 890, 1050 Å$^2$) calculated using the size of the colipase (25 × 30 × 35 Å) in the lipase/colipase complex (*31*). This discrepancy simply results from the partial dissolution of the colipase in the subphase. Then, the spread colipase monolayer was compressed by moving the Teflon barriers to obtain a lateral pressure of 10 mN/m. As shown in Figure 1B, the colipase monolayer is still relatively stable, with a mean surface area of 590 Å$^2$/molecule (Figure 1A). By contrast, when the film was further compressed to reach a lateral pressure of 18 mN/m, the film of colipase was not fully stable as revealed by the continuous decrease of the trough area to maintain the surface pressure constant (Figure 1B). As well, the mean surface area of colipase at 18 mN/m decreases from 510 Å$^2$/molecule to about 489 Å$^2$/molecule in 2000 s (Figure 1A). The decrease of the apparent molecular area of colipase with the surface pressure can result either from a reduction of the distance between the colipase molecules at the interface, a desorption of molecules from the film, or the formation of colipase aggregates. However, the relative stability of the film at lateral pressure 10 mN/m (Figure 1B) and the apparent molecular area value closed to those of the crystalline colipase indicate that, at this surface pressure, most of the protein remains at the air/water interface even if the equilibrium is metastable. By contrast, at higher lateral pressure, a desorption process seems more likely to explain the decrease of the molecular area since colipase, soluble in water, will rather form a Gibbs monolayer than a Langmuir monolayer. The PM-IRRAS spectra below will give complementary information.

The structure and orientation of colipase at the air/buffer interface was investigated by PM-IRRAS. Although colipase can be considered as a soluble surfactant that may partition between the interface and the bulk, the bulk concentration of colipase was so weak that the PM-IRRAS measurements will be sensitive only to the colipase present at the interface. The PM-IRRAS spectra of the colipase film were collected at the three different pressures. Since the recording time for all PM-IRRAS spectra were around 300 s, the influence of the instability of the colipase film at 18 mN/m on the PM-IRRAS spectrum is negligible. As shown in Figure 1C, all of them displayed two well defined but quite broad amide bands, confirming the presence of the colipase at the interface at all lateral pressures. The intensification of both the amide I and II bands when the lateral pressure increased suggests a progressive increase of colipase concentration under the IR beam. However, the intensity of the PM-IRRAS spectra is proportional to both the concentration of molecules at the interface and the orientation function of each vibration: $I = (N_i/A_i) \times N_j(\theta)$, ($N_i$, molecule number at the area interface ($A_i$) and $F_j(\theta)$, orientation function). The PM-IRRAS signal can be normalized by multiplying each PM-IRRAS spectrum by its corresponding $A_i$, using the above formula. The PM-IRRAS signal thus becomes proportional to the orientation function and the number of molecules.

The secondary structure of colipase at the air/buffer interface can be estimated from the frequency position and intensity of the amide bands. Irrespective of the lateral pressure, the deconvolution of the amide I (C═O stretching) band reveals a major contribution of α-helix (1656 cm$^{-1}$) and random coil (1640 cm$^{-1}$) structures and to a lesser extent to $\beta$-sheet (1630 and 1670 cm$^{-1}$) (*32*, *33*). As shown in Figure 1C, the global shape of the amide I band remained unchanged with increasing lateral pressure, which means that the secondary structure of colipase is mainly pressure independent between 1 and 18 mN/m. The amide II band (coupling of NH bending and CN stretching) was centered at 1520 cm$^{-1}$ at 1 mN/m but broadened toward higher wavenumbers (1540 cm$^{-1}$) upon compression of the film. Moreover, the amide I/amide II intensity ratio, which is indicative of the protein orientation at an interface, was close to 1.1 at all pressures. This value suggests that colipase keeps the same orientation at all lateral pressures with the average mean axis of the CO amide groups of the various structure (helix, $\beta$-sheet, random) tilted on the plane (*24*, *34*).

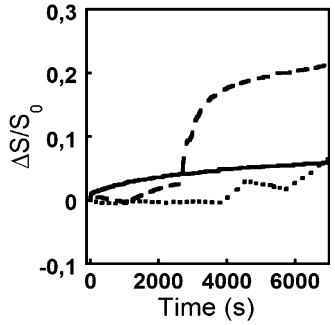


FIGURE 2: Kinetics of colipase adsorption on different lipid monolayers, $\Pi = 20$ mN/m (- - -) pure dilaurin; (—) L-α-PC monolayer, (•••) mixed 70% L- α-PC/30% dilaurin (mol/mol). Addition of 33 nM colipase was done at 2600 s for dilaurin, 200 s for L-α-PC, and 4000 s for the mix. Subphase: 10 mM Tris-HCl buffer containing 100 mM NaCl and 5 mM $CaCl_2$ pH 7.5.

Moreover, since the orientation function is almost the same during the colipase film compression, the PM-IRRAS signals will be proportional only to the number of molecules. Using the above normalization on the spectra presented in Figure 1C, the calculation shows that the normalized signals are almost constant at 1.1 and 10 mN/m but slightly decrease at 18 mN/m. These results indicate that the number of colipase molecules present at the interface at 1 and 10 mN/m is roughly the same while at 18 mN/m the number of colipase molecules decreases. This variation indicates that the reduction of the apparent surface area of colipase with the surface pressure is likely due to a condensation of the colipase at 10 mN/m and a partial desorption at 18 mN/m.

*Kinetics of Colipase Adsorption at Different Lipid Interfaces.* Colipase adsorption on the three types of buffer/lipid interfaces was investigated at a constant lateral pressure of 20 mN/m. As shown in Figure 2, the kinetics of adsorption were different depending on the lipid species present at the interface, and the recording times depend upon the area through stabilization.

Injection of colipase under a dilaurin interface induced an 18% global increase of the trough area (Figure 2a). A two-step process was observed with a rapid increase of the surface pressure resulting in the opening of the barriers to maintain constant pressure, followed by a slower process. This relatively high increase indicated a deep insertion of colipase into the dilaurin monolayer. Figure 2a also demonstrates an instability of the pure dilaurin film as revealed by the decrease of the trough area before colipase injection (0−1000 s). Such a profile suggests that dilaurin molecules at this temperature have a natural propensity to form aggregates.

By contrast, adsorption of colipase to an L-α-PC monolayer resulted in a progressive and rather weak increase of the trough area (Figure 2c). This relative area increase (4%) was significantly lower than that observed with dilaurin (18%). This means that colipase does not fully penetrate the L-α-PC monolayer and that the insertion is partial, probably at the polar head group level.

The profile of the adsorption kinetic at a mixed 70% L-α-PC/30% dilaurin (mol/mol) was somewhat different from those obtained with dilaurin or L-α-PC. Indeed, the presence of colipase induced only a slow and weak increase of the trough area (Figure 2b). The adsorption process is much slower than that observed with the dilaurin monolayer, and

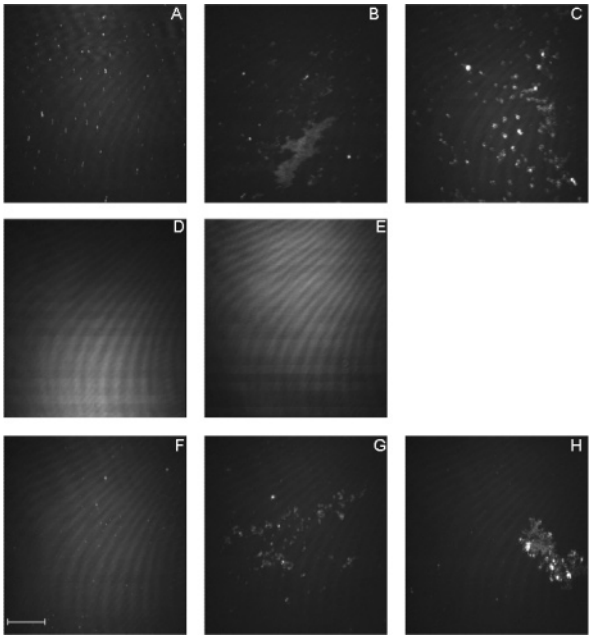


FIGURE 3: BAM images of lipid monolayers in the absence or presence of colipase. A, B, C: dilaurin, $\Pi = 18$ mN/m; D, E: L-α-PC, $\Pi = 22$ mN/m; F, G, H: 70% L-α-PC/30% dilaurin (mol/mol), $\Pi = 18$ mN/m. (A) pure dilaurin: GL = 47; OS = 50; $R = 34.6 \times 10^{-8}$. (B) $t = 20$ min after colipase injection: GL = 46; OS = 120; $R = 42.9 \times 10^{-8}$. (C) $t = 25$ min after colipase injection: GL = 33; OS = 120; $R = 43.9 \times 10^{-8}$. (D) L-α-PC; GL = 65; OS = 50; $R = 58.3 \times 10^{-8}$. (E) $t = 23$ min after colipase injection; GL = 98; OS = 50; $R = 111 \times 10^{-8}$. (F) Mixed lipids; GL = 56; OS = 50; $R = 47.4 \times 10^{-8}$. (G) $t = 15$ min after colipase injection; GL = 40; OS = 120; $R = 59.6 \times 10^{-8}$. (H) $t = 25$ min after colipase injection; GL = 39; OS = 120; $R = 55.5 \times 10^{-8}$. Subphase: 10 mM Tris-HCl buffer containing 100 mM NaCl and 5 mM $CaCl_2$ pH 7.5. $[\text{Colipase}]_{\text{subphase}} = 14$ nM; GL = gray level; OS = obturation speed; $R$ = reflectivity. The scale bar in image *F* is 87 $\mu$m and is appropriate for all images.

at 6000 s, a stabilization of the adsorption process was still not reached. At this stage, the global increase (9%) of the trough area, intermediate between 4% (L-α-PC) and 18% (dilaurin), suggests that the insertion of colipase is not as deep as that observed with dilaurin. The mixed L-α-PC/dilaurin monolayer is stable as compared to the dilaurin monolayer, which means that there is no spontaneous condensation of the lipids.

*BAM Study of the Morphology of Mixed Colipase/Lipid Monolayers.* The morphology of lipid alone and mixed lipid/colipase monolayer was investigated by BAM at constant lateral pressure of 18 mN/m for dilaurin and L-α-PC/dilaurin monolayer and 22 mN/m for L-α-PC. BAM images were acquired as a function of time before and after injection of colipase beneath the different lipid monolayers. As shown in Figure 3A,D,F, the BAM images of the lipid monolayers differed according to the lipid species. With L-α-PC and 70% L-α-PC/30% dilaurin (Figure 3D, F), the lipid monolayer was in a homogeneous liquid condensed phase. With dilaurin (Figure 3A), some bright spots, characteristic of a phase separation of the lipids with condensed domains, were observed. These BAM images of the dilaurin monolayer confirmed the propensity of dilaurin to form aggregates as suspected from the decrease of surface pressure observed in Figure 2a.

When colipase was injected underneath the dilaurin monolayer, the bright spots observed with dilaurin alone

grow in size with time (Figure 3B,C). A progressive increase of the average normalized reflectivity was observed, a behavior characteristic of lipid regions more concentrated in colipase (Figure 3B,C). The average gray level reflectivity, and thus reflectance, increased from $3.34 \times 10^{-7}$ to $12.7 \times 10^{-7}$ in the less bright domains and to $17.1 \times 10^{-7}$ in the brighter zones (Figure 3A,B). With time (Figure 3C), the reflectance of the brighter aggregated domains was $19.6 \times 10^{-7}$. From these data, the thickness of the dilaurin monolayer (Figure 3A) was estimated to 13 Å using the BAM software and a refractive index of 1.43 for liquid expanded phase. With the same refractive index, the increase of thickness in the aggregated domains in the presence of colipase was estimated to vary from 10 to 14 Å in Figure 3B and from 14 to 16 Å in Figure 3C. We can notice that these increases were smaller than the minimal dimension of colipase ($25 \times 30 \times 35$ Å).

With L-α-PC, no condensed domains were observed upon colipase injection, even after a long time (Figure 3E). However, the average reflectivity increased from $5.83 \times 10^{-7}$ to $11.1 \times 10^{-7}$. This change is characteristic of both an average thickness and refractive index increase at the interface consecutive to colipase adsorption. Using the BAM software and refractive indexes of 1.45 and 1.47 for L-α-PC and colipase, respectively, the thickness of the layers was estimated at 14 Å for the L-α-PC monolayer and 18.5 Å in the presence of colipase. These values are in agreement with a slight insertion of colipase in the phospholipid monolayer.

As shown in Figure 3G and 3H, a clear change in the morphology of the mixed 70% L-α-PC/30% dilaurin monolayer was observed upon colipase addition, with the apparition of bright condensed domains, similar to those observed in the case of dilaurin and colipase. The reflectivity increased from $5.7 \times 10^{-7}$ to $21.5 \times 10^{-7}$ in the less bright condensed domains and to $50.3 \times 10^{-7}$ in the brighter zones. From these data, the thickness of the layers was estimated to 13 Å for the mixed L-α-PC/dilaurin monolayer, 24 Å for the less bright colipase/lipid domains, and 37 Å for the brighter zones using a refractive index of 1.45 for the mixed lipids. The thickness of the brighter domains (37 Å) is equivalent to the dimensions of colipase ($25 \times 30 \times 35$ Å), suggesting that, in these aggregates, a monolayer of colipase is formed under the lipids. If we correlate these results to those observed with L-α-PC and dilaurin, we can propose that the condensed domains are made of colipase and dilaurin molecules because no aggregates have been observed with L-α-PC in the presence of colipase.

*Colipase-Induced Lipid Perturbations by PM-IRRAS.* Lipid perturbations induced by protein adsorption can be conveniently monitored through the frequency of the $\nu(CH_2)_{s,as}$ stretching vibrations, characteristic of the acyl chain conformation. It is now well known that values lower than 2850 $cm^{-1}$ for $\nu(CH_2)_s$, and 2920 $cm^{-1}$ for $\nu(CH_2)_{as}$ indicate chains with rather high conformational order whereas values higher than 2850 and 2920 $cm^{-1}$ indicate the presence of gauche bonds (*35*). Moreover, the frequency of the lipid C═O ester gives information on the water accessibility of this functional group. The frequency of the maximum slightly decreases when this group is more accessible to water to form hydrogen bonds.

The PM-IRRAS spectra were recorded at 20 mN/m for each type of monolayer and at different times after colipase injection during the kinetic of adsorption. The perturbation induced by the adsorption of colipase on the lipids was investigated using the PM-IRRAS spectrum of the subphase as standard.

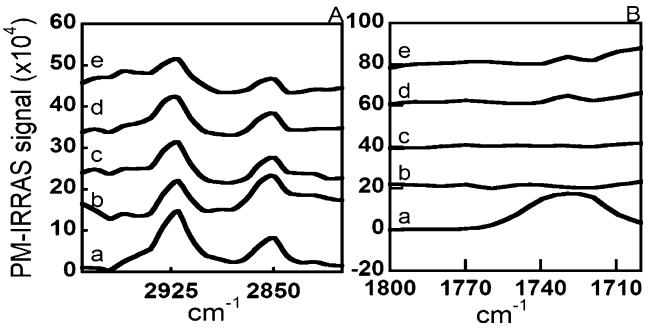


FIGURE 4: Normalized PM-IRRAS spectra of the lipid perturbations induced by colipase in interaction with a dilaurin monolayer, $\Pi$ = 20 mN/m. (A) $\nu CH_2$ region (2850−2950 $cm^{-1}$); the spectra were divided by that of the subphase. (B) C═O ester band vibration (1700−1800 $cm^{-1}$); the spectra were divided by that of the pure lipid. (a) dilaurin monolayer, (b) $t$ = 7 min after colipase injection, (c) $t$ = 24 min, (d) $t$ = 49 min, (e) $t$ = 82 min. $[Colipase]_{subphase}$ = 33 nM; subphase: 10 mM Tris-HCl buffer pH 7.5 containing 100 mM NaCl and 5 mM $CaCl_2$.

PM-IRRAS measurements of dilaurin monolayer at $\pi$ = 20 mN/m showed vibration bands at 2852, 2921, and 1727 $cm^{-1}$ due to the $\nu(CH_2)_{s,as}$ and $\nu$(C═O) ester stretching vibrations, respectively (Figure 4Aa, Ba). Injection of colipase under the dilaurin monolayer induced a clear perturbation of the lipid chain. The intensity of the $\nu(CH_2)_{s,as}$ stretching bands at 2852 $cm^{-1}$ and 2921 $cm^{-1}$ decreased (Figure 4A) and a shift toward the higher wavenumbers (2921→2924 $cm^{-1}$; 2852→2853 $cm^{-1}$) was noted for both $\nu(CH_2)$ bands. These two phenomena are actually connected since an increase in the proportion of gauche conformation increases the average tilted angle of the acyl chains which, in turn, decreases the PM-IRRAS signal of the $CH_2$ absorption (*24*). The $\nu$(C═O) ester band showed few perturbation soon after colipase injection (7 min), but with time this band slowly increased and appeared positive relative to the baseline, suggesting a change in the orientation of the C═O ester groups (Figure 4B). From the selection rule of PM-IRRAS (see Materials and Methods), we can deduce that the C═O lipid groups tend to be preferentially in the monolayer plane. Moreover, the shift of the $\nu$(C═O) ester band toward the higher frequencies (1729 $cm^{-1}$) is indicative of the dehydration of the carbonyl group with a decrease in the proportion of hydrogen-bonded carbonyl.

The L-α-PC monolayer is characterized by bands at 2854, 2922, 1730, 1090 with a shoulder at 1060 $cm^{-1}$ and 1224 $cm^{-1}$ due to the $\nu(CH_2)_{s,as}$, $\nu$(C═O) ester and $(PO_2^-)_{s,as}$ groups, respectively (Figure 5Aa, Ba, Ca). As observed with dilaurin, the intensity of the $\nu(CH_2)_{s,as}$ bands (2854 and 2922 $cm^{-1}$) progressively decreased with time (Figure 5A) after injection of colipase beneath the L-α-PC film. The 2854 $cm^{-1}$ band slightly shifted toward higher frequencies (2855 $cm^{-1}$), indicating an increase in gauche conformation which thus gives a more fluid lipid layer. The perturbation induced by colipase adsorption on the $\nu$(C═O) ester band at 1730 $cm^{-1}$ (Figure 5B) was very low, but a slightly negative band can be noted with a shift toward higher frequencies (1733 $cm^{-1}$). This suggests an interaction between colipase and the L-α-PC molecules, which induces a change in the orientation of

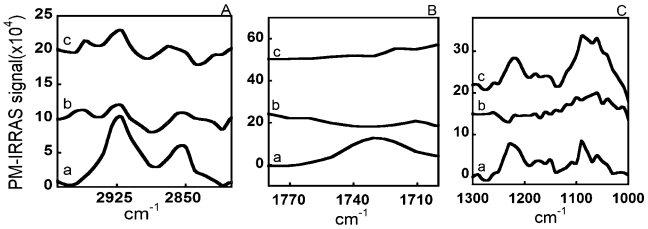


FIGURE 5: Normalized PM-IRRAS spectra of the lipid perturbations induced by colipase in interaction with a L-α-PC monolayer, $\Pi$ = 20 mN/m. (A) $\nu CH_2$ region (2850−2950 $cm^{-1}$). (B) C═O ester band vibrations (1700−1800 $cm^{-1}$); the spectra were divided by that of the pure lipid; (C) $\nu(PO_2^-)$ region. For A and C, the spectra were divided by that of the subphase. (a) L-α-PC monolayer, (b) $t$ = 34 min after colipase injection, (c) $t$ = 84 min. $[Colipase]_{subphase}$ = 33 nM; subphase: 10 mM Tris-HCl buffer pH 7.5 containing 100 mM NaCl and 5 mM $CaCl_2$.

the lipid chain near the ester group. However, the main changes occurred in the 1100−1200 $cm^{-1}$ region, characteristic of the $PO_2^-$ region (Figure 5C). While in the absence of colipase the [1060−1090 $cm^{-1}$] and 1224 $cm^{-1}$ contributions were somewhat similar, the adsorption of colipase onto the L-α-PC monolayer induced a broadening of the 1060−1090 $cm^{-1}$ contribution toward lower frequencies and a shift of the 1224 $cm^{-1}$ band toward lower frequencies (1220 $cm^{-1}$). Moreover, with time, the 1060−1090 $cm^{-1}$ band, characteristic of the $PO_2^-$ symmetric stretch, became predominant.

The PM-IRRAS spectrum of the mixed 70% L-α-PC/30% dilaurin monolayer displayed bands at 2854, 2922, 1733, 1227, and 1089 with a shoulder at 1061 $cm^{-1}$ corresponding to the $\nu(CH_2)_{s,as}$, $\nu$(C═O) ester, and $PO_2^-$ groups, respectively (Figure 6Aa, Ba, Ca). In the $\nu(CH_2)_{s,as}$ region, the spectra were very similar to that of the lipid mix alone (Figure 6A), except for a shift of the 2854 $cm^{-1}$ band to lower frequencies (2851 $cm^{-1}$). This shift is indicative of a conformational ordering of the lipid acyl chains induced by the presence of colipase. As previously observed with the L-α-PC monolayer, the adsorption of colipase at the interface of the monolayer did not induce any significant perturbation of the C═O ester band (Figure 6B). As for L-α-PC monolayer, the most important perturbations were observed in the $PO_2^-$ region (Figure 6C). While the 1090 $cm^{-1}$ contribution ($PO_2^-$ symmetric stretch) was predominant in the mixed lipid monolayer spectrum, the adsorption of colipase resulted in an inversion of the relative band intensities since the 1227 $cm^{-1}$ band ($PO_2^-$ antisymmetric stretch) became predominant with time. The frequency position of this band remained almost the same, which indicates that the phosphate should have the same environment before and after the colipase injection.

*Analysis of the Structure of Colipase Bound to Lipid Monolayers.* The presence of colipase at the different water/lipid interfaces can be visualized through the amide band contributions and its structure deduced from changes in these contributions. The orientation and conformation of colipase at the interface was studied using the PM-IRRAS spectrum of lipid alone as the standard.

As shown in Figures 7A−C, in all cases, the presence of colipase was confirmed by the amide signals. However, the difference in the relative intensities of the amide bands suggests a lower amount of colipase present at the mixed phospholipid/dilaurin interface as compared to that present at the dilaurin interface.

The spectra of colipase under the dilaurin monolayer (Figure 7A) are very different from that of colipase at the air/buffer interface at $\pi$ = 18 mN/m which displays two well-defined amide I and II bands centered at 1656 and 1540 $cm^{-1}$, respectively. This means that the protein is likely to adopt a different structure and orientation during its adsorption on dilaurin. At the beginning of the adsorption process on the dilaurin monolayer, the signals of both the amide I and II were weak and the bands were not well defined. With time, the amide I band became predominant with a positive contribution around 1670 $cm^{-1}$ characteristic, most of the time, of $\beta$-turn structures and a negative contribution centered at 1620 $cm^{-1}$ characteristic of an antiparallel $\beta$-sheet. The intensification of these two contributions with time is correlated with the progressive increase of colipase concentration under the IR beam. The negative contribution observed for the amide I band around 1620 $cm^{-1}$ suggests, based on the PM-IRRAS selection rule, that the C═O amide direction of the antiparallel $\beta$-sheet chains should be mainly perpendicular to the plane of the interface. Broadening of the 1620 $cm^{-1}$ band toward lower wavenumbers is a spectral modification that can be produced by perturbation of the interfacial water. Concomitantly, a progressive disappearance of the amide II band is observed.

As well, colipase at the L-α-PC interface displayed a PM-IRRAS spectrum different from that observed at the air/buffer interface, indicating that the protein does not have the same conformation (Figure 7B). At 34 min time of adsorption, a unique, nondefined band centered at about 1630 $cm^{-1}$ is visible, indicating the presence of antiparallel $\beta$-sheet structures. With time, the spectrum changed and displayed a broad amide I band centered around 1650 $cm^{-1}$ and an

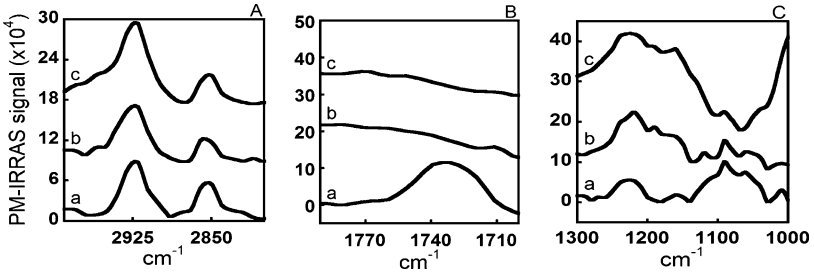


FIGURE 6: Normalized PM-IRRAS spectra of the lipid perturbations induced by colipase in interaction with a 70% L-α-PC/30% dilaurin monolayer. $\Pi$ = 20 mN/m. (A) $\nu CH_2$ region (2850−2950 $cm^{-1}$). (B) C═O ester band vibrations (1700−1800 $cm^{-1}$); the spectra were divided by that of the pure lipid. (C) $\nu(PO_2^-)$ region. For A and C, the spectra were divided by that of the subphase. (a) Mixed lipid monolayer, (b) 22 min after injection of colipase, (c) 45 min. $[Colipase]_{subphase}$ = 40 nM; subphase: 10 mM Tris-HCl buffer pH7.5 containing 100 mM NaCl and 5 mM $CaCl_2$.

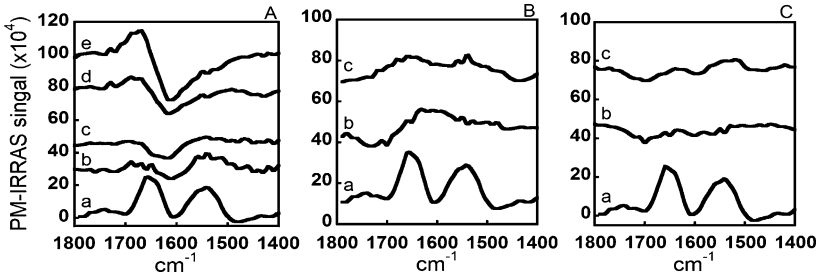


FIGURE 7: Amide region of the normalized PM-IRRAS spectra of colipase in interaction with lipid monolayer, $\Pi = 20$ mN/m. (A) Dilaurin monolayer: (a) colipase at the air−water interface, (b) $t = 7$ min after colipase injection, (c) $t = 24$ min, (d) $t = 49$ min, (e) $t = 82$ min. (B) L-α-PC monolayer: (a) colipase at the air−water interface, (b) $t = 34$ min after colipase injection, (c) $t = 84$ min. (C) 70% L-α-PC/30% dilaurin monolayer: (a) colipase at the air−water interface, (b) 22 min after injection of colipase, (c) 45 min. All the spectra were divided by that of the lipid. $[\text{colipase}]_{\text{subphase}} = 33$ nM; subphase: 10 mM Tris-HCl buffer pH 7.5 containing 100 mM NaCl and 5 mM $CaCl_2$.

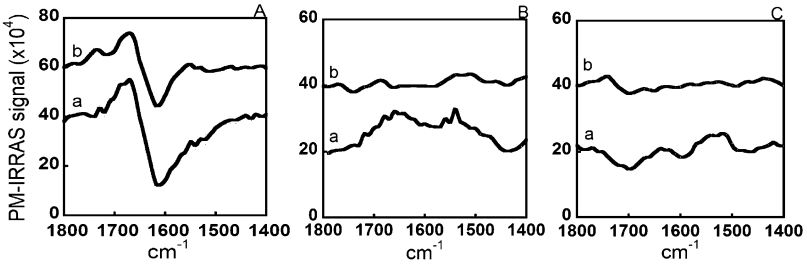


FIGURE 8: Amide region of the normalized PM-IRRAS spectra of colipase in interaction with lipid monolayer, $\Pi = 30$ mN/m. (a) Surface pressure $\Pi = 20$ mN/m, (b) surface pressure $\Pi = 30$ mN/m. (A) Dilaurin monolayer. (B) L-α-PC monolayer. (C) 70% L-α-PC/30% dilaurin monolayer. All the spectra were divided by that of the lipid. $[\text{Colipase}]_{\text{subphase}} = 33$ nM; subphase: 10 mM Tris-HCl buffer pH 7.5 containing 100 mM NaCl and 5 mM $CaCl_2$.

amide II band centered at 1540 cm$^{-1}$. These band shapes and the amide I position were characteristic of both disordered and $\beta$-sheet structures. Moreover, the intensity ratio ($r$) of the amide I/amide band ($\sim$1.6) is close to the value obtained for isotropic proteins in solution (*28*). All these observations (broad band and $r$ value) suggest that colipase interacts with a nonpreferred orientation to the L-α-PC interface. The presence of colipase at the interface of the mixed 70% L-α-PC/30% dilaurin is confirmed by the amide contributions (Figure 7C) where the amide I band is centered at 1633 cm$^{-1}$, characteristic of $\beta$-sheet structures. Moreover, the shoulder at higher frequency can be assigned to the random coil structure. During the adsorption time, we observed a very significant increase of the amide II band intensity centered at 1530 cm$^{-1}$ relative to the intensity of the amide I. As a consequence, the amide I/amide II intensity ratio on the final spectrum is low and close to 1. Taking into account the selection rule of the PM-IRRAS, this indicates that the $\beta$-sheet structures are oriented with the C═O of the amide groups largely out of the interface plane.

The same experiments were performed at a lateral pressure of 30 mN/m (Figure 8). In the case of pure lipids, the colipase is still present at the interface but at a lower concentration as revealed by the weak band intensities on the PM-IRRAS spectra. By contrast, the presence of colipase was not detectable at the mixed dilaurin/ L-α-PC interface at such lateral pressure.

## DISCUSSION

One of the main functions of colipase is to facilitate the lipase-catalyzed lipid hydrolysis by anchoring the lipase at the lipid droplets interface coated with biliary lipids. This implies for both proteins an ability to interact with lipids such as phospholipids, fatty acids, and lipase substrates. A great deal of information has been obtained by Brockman and co-workers who studied the interaction of colipase with various lipid monolayers in different conditions (pH, salt concentration) (*20*, *36*, *37*). They analyzed the lipid composition dependence of colipase adsorption and showed that colipase exhibits a clear specificity for interface containing lipolysis reactants (fatty acids, tri- and diacylglycerol) (*20*). Lipid−colipase nanodomains made of one colipase molecule and 20 to 30 reactant acyl chains (*38*) would then be formed at the interface. By contrast, phospholipids, in particular their hydrated polar head, would rather act as sites preventing colipase adsorption. As well, they have shown that lipolysis reactants (diglyceride or fatty acid) also decreased the colipase adsorption rate when 1-stearoyl-2-oleoyl-sn-glycero-3-phosphocholine (SOPC) is present (*37*). One explanation given for this observation is that SOPC and the reactants form dynamic complexes which, as for SOPC alone, preclude colipase binding (*37*). Thus, by controlling the concentrations of these lipids at its vicinity, colipase would regulate the concentration of lipase at the interface (*36*). Using colipase adsorption as a model, Sugar et al. (*39*) elaborated a model, the free-area model, in which parts of the hydrocarbon tails of the phospholipids could become exposed when their specific area increased, thus forming the hydrophobic area (headgroup free) to which colipase will bind preferentially.

In this work, we have combined for the first time both PM-IRRAS and BAM approaches to visualize the impact of colipase on different monolayers and to study its orientation in situ.

*Colipase Structure at the Air/Buffer Interface.* The behavior of colipase at the air/water interface was investigated to obtain a global picture of the conformation and orientation

of colipase at a hydrophobic/hydrophilic interface. The adsorption isotherm shows that, although colipase is a water soluble protein and will rather form a Gibbs monolayer than a Langmuir monolayer, it displays a good affinity for the air/water interface and that adsorption of colipase at the air/water interface does not cause its denaturation, as previously reported by Momsen et al. (*36*). At all pressures tested (1, 10, and 18 mN/m), the colipase keeps almost the same structure, with a major contribution of α-helix and *β*-sheet structures. Interestingly, the three-dimensional structure of colipase reveals only two short α-helical stretches (*11*, *12*), one of them being observed only in the presence of lipase and amphipathic compounds in the crystallization medium. From the amide I/amide II intensity ratio (*1*, *1*), which remains roughly the same at all pressures, we can deduce, from our previous work (*24*), that colipase also keeps the same orientation with the average mean axis of the amide group including α-helical structure tilted at ∼40° to the normal at the interface. Analysis of the colipase film stability upon compression reveals that the film is rather stable up to 10 mN/m but becomes unstable at 18 mN/m. This observation, correlated to the fact that colipase retains the same orientation, strongly suggests that colipase has a propensity to form condensed phase at the interface between 1 and 10 mN/m, but at higher pressure (18 mN/m), a desorption process is more likely.

Since colipase is devoted to interact with biliary and dietary lipids, it was relevant to study its secondary structure and its orientation at water/lipid interfaces as well as the impact of its adsorption on the lipids. Lipids mimicking the lipids found at the surface of the dietary lipid droplet surface were used in this study. L-α-PC was used for mimicking the biliary phospholipids which mainly consist of phosphatidylcholine (*40*) and mixed isomers 1,2 and 1,3 dilaurin to mimic the lipase substrate. A mixed L-α-PC/dilaurin monolayer containing 30% of dilaurin was also used as model of the lipid droplet surface. The PM-IRRAS investigations were combined with BAM to also analyze the morphology of lipid and mixed colipase/lipid monolayers. The BAM images reveal that, while the L-α-PC and 70% L-α-PC/30% dilaurin monolayers are in a homogeneous liquid condensed phase, the dilaurin monolayer is heterogeneous with the presence of small domains, indicating that dilaurin molecules tend to spontaneously form condensed domains. The kinetics of colipase adsorption clearly show that colipase displays a different behavior depending on the lipid species present at the interface.

*Colipase Structure at a Dilaurin Interface and Lipid-Induced Perturbations.* Colipase penetrates deeply into a dilaurin film and promotes the formation of protein/lipid domains as visualized on the BAM images. This is a feature specific to colipase since no increase of the number and thickness of dilaurin aggregates was observed when lipase was injected in the subphase (data not shown). The estimated thickness of the domains lower than the minimal dimension of colipase (20 × 30 × 35 Å) confirms the insertion of colipase and suggests that the protein is either dispersed among the dilaurin molecules or surrounds the aggregates. From the unique PM-IRRAS spectral shape of colipase, it is clear that the protein adopts a peculiar orientation under this lipid monolayer, even if we cannot describe it precisely. Insertion of colipase disturbs the organization of the lipid acyl chains, inducing an increase in gauche conformation resulting in a more tilted average angle of the carbon chains. In the condensed domains, colipase interacts with the lipid C═O ester groups which are likely orientated in the monolayer plane and with the acyl chain via hydrophobic interactions. The domains observed in the BAM images result from those interactions. Moreover, a dehydration of the carbonyl group of dilaurin is observed in agreement with Sugar et al. (*41*) who suggest that diacylglycerols form, at an interface, transient, partly dehydrated clusters which act as sites for the initial binding of colipase to the interface. The two-step adsorption observed in the kinetic can be correlated to the PM-IRRAS spectra of the colipase. The evolution of the PM-IRRAS spectra of the colipase with time is also really specific and indicates a progressive change in the colipase orientation at the dilaurin interface, since the amide I and II bands, positive at the beginning of the adsorption process, change to give a negative amide I component and a weak amide II at the end of the adsorption. The main structural elements of colipase involved in the interaction with dilaurin molecules are *β*-turns and antiparallel *β*-sheet structures preferentially orientated out of the plane. This behavior is different from that observed at the air−water interface. It should be mentioned that the possibility of an aggregation of colipase under the lipid monolayer should also be considered since the 1620 $cm^{-1}$ contribution has also been assigned by some authors to intermolecular hydrogen-bonded *β*-sheets (*42*, *43*).

*Colipase in an* L-α-*PC Environment: Lipid Perturbation and Colipase Orientation.* In an L-α-PC environment, colipase behaves differently. The small but continued increase in lateral pressure in the course of colipase adsorption is the sign of a progressive but partial insertion of colipase. In contrast to what was observed with dilaurin, this partial insertion does not result in the formation of lipid or lipid/colipase aggregates as revealed by the absence of bright spots on the BAM images. However, the significant increase in the luminosity of the images and the PM-IRRAS spectra confirms the presence of colipase at the L-α-PC interface. The main lipid perturbations observed upon colipase adsorption are located in the region characteristic of the polar head group (1250−800 $cm^{-1}$), supporting the idea of a partial insertion of colipase restricted to the polar head of the phospholipids. The changes in the $PO_2^-$ region reveal that colipase interacts with these groups via hydrogen bonds (*44*, *45*), and that these interactions induce a reorientation of the $PO_2^-$ group. The structure of colipase also evolved with time. At first, antiparallel *β*-sheets seemed to be the major structural elements involved in the interaction with the phospholipids. Then, the width and position of the amide I band were consistent with the predominant contribution of random coil structures in the L-α-PC/colipase interaction. Interestingly, the broad band shape and the amide I/amide II intensity ratio close to 1.7 indicates a quasi-isotropic orientation of colipase at the interface. This latter result is of particular interest since Ayvazian et al. (*30*) have shown that colipase presumably functions by controlling the proper orientation of the active ternary complex (lipase/colipase/micelle) at the oil−water interface. An isotropic orientation could explain why colipase is not able to counteract the inhibitory effect of phospholipids on the lipase activity, thus reinforcing the idea that colipase requires a precise and

peculiar orientation at the lipid interface to properly function. It must be pointed out, however, that the isotropic orientation is a global image of the protein orientation which does not exclude that some structural elements, such as those interacting with the polar head of the lipid, maintain a preferential orientation toward the lipid interface.

*Structure and Orientation of Colipase at a Mixed 70% L-α-PC/30% Dilaurin Interface.* To investigate the behavior of colipase in a more physiological environment, we used a mixed 70% L-α-PC/30% dilaurin (mol/mol) monolayer to mimic the surface of the lipid droplets. It is interesting to note that despite the presence of dilaurin which, alone, spontaneously forms aggregates, the mixed film is stable and displays a homogeneous surface with no bright spots, characteristic of miscible lipids in a liquid condensed phase. The presence of colipase induces a reorganization of the resulting film visualized by the BAM images which clearly show that colipase triggers the formation of bright domains or aggregates with a thickness of 24 to 37 Å. The fact that no aggregation was observed with L-α-PC supports the idea that the bright domains are mainly formed by colipase and dilaurin molecules which means that colipase recruits dilaurin molecules. The estimated thickness of the more condensed domains (37 Å) which is equivalent to the dimensions of colipase (25 × 30 × 35 Å) strongly supports that colipase does not insert into the dilaurin molecules as with the pure diglyceride but rather forms a uniform monolayer under the aggregates. The L-α-PC molecules appear totally excluded from these domains. These results are in agreement with the colipase specificity for lipolysis reactants described by Brockman et al. (*20*) and with the lateral redistribution of diglycerides proposed by Sugar et al. (*37*). One surprising feature is that colipase adsorption to the mixed monolayer induces perturbations on the lipid acyl chains opposite to those observed with dilaurin alone since a conformational ordering of the acyl chains is observed. The effect observed in the region of the $PO_2^-$ asymmetric stretch (1220−1250 $cm^{-1}$) contribution, a frequency sensitive to ion binding and/or hydration, means that adsorption of colipase also induces a reorientation of the $PO_2^-$ group, which becomes more exposed to the solvent. However, the fact that the band frequency is almost the same during colipase adsorption gives evidence that colipase does not interact strongly with L-α-PC. From the PM-IRRAS spectra of colipase, the structural elements involved in the colipase/lipid interactions are mostly random and $\beta$-sheet structures. It also clearly appears that colipase undergoes a change of orientation at the mixed L-α-PC/dilaurin as shown by the final spectrum shape, characterized by a weak depression around 1665 $cm^{-1}$ and an amide I band with almost the same intensity as the amide II band ($R_{\text{amide I/amide II}} \approx 1$). Such spectral shapes are observed, in the case of the helix structure, when the amide C═O groups are largely out of the interface plane as described by Cornut et al. (*24*). The description of the $\beta$-sheet with respect to the interface plane is more complicated because two angles are necessary. Recently, we performed new calculations that show that the $\beta$-sheet structures present a similar PM-IRRAS response concerning the C═O amide orientation (personal data). Briefly, the amide I/amide II ratio decreases from 2.57 to −3 when the $\beta$-sheet shifts from an interface plane orientation to a perpendicular orientation with the amide C═O vertical. In the case of an isotropic orientation, the amide I/amide II ratio is around 1.7. In our case, the amide I/amide II ratio is equal to 0.93, and the best fit to the simulations corresponds to an average tilt of 60° and 45° for the C═O amide group and the peptide chains, respectively.

We also looked at the colipase adsorption at a lateral pressure of 30 mN/m, which is thought to coincide with the lateral pressure in the membrane (30−32 mN/m) (*46*). It clearly appears that colipase is still present at the lipid interface in the case of pure lipids (dilaurin and L-α-PC) although at a lower amount than at 20 mN/m. Our results with L-α-PC monolayer are in discordance with those of Momsen et al. (*20*) who showed that colipase adsorption is fully inhibited at surface pressure above 24 mN/m. This discrepancy could be explained by a difference of sensitivity of the techniques used. Momsen and co-workers used surface pressure techniques which are very sensitive for insertion or desorption processes but fail to detect a protein adsorbed just underneath the surface. By contrast, no colipase was detected at the mixed dilaurin/ L-α-PC interface at 30 mM/m. This would mean that dilaurin molecules are no longer available to bind colipase and that the phosphate groups display an orientation unfavorable to colipase adsorption. To explain this behavior at this lipid ratio and lateral pressure, one can propose that the polar heads of L-α-PC are likely to spread out at the water/lipid interface, giving a peculiar orientation of the phosphate groups and shielding the dilaurin molecules.

In conclusion, combining PM-IRRAS and BAM studies allow us to determine for the first time the orientation and structure of colipase at different water/lipid interfaces and to demonstrate the lipid perturbations induced by its adsorption. We show that dilaurin, a lipase model substrate, and colipase have a natural propensity to segregate and form aggregate or domains at the air/water interface. Mixed together both molecules will interact to form larger domains in which colipase is not uniformly distributed. We also show that colipase partially penetrates into L-α-PC monolayer but with a nonpreferred orientation. This nonspecific behavior could be responsible for its inability to restore lipase activity in the presence of phospholipids. At a mixed L-α-PC/dilaurin interface, colipase also triggers the formation of dilaurin clusters excluding the L-α-PC molecules but does not really interact with either lipid species. Colipase adsorbs to the resulting dilaurin aggregates with a specific orientation but does not penetrate deeply into the lipid monolayer.

## REFERENCES

1. Carriere, F., Laugier, R., Barrowman, J. A., Douchet, I., Priymenko, N., and Verger, R. (1993) Gastric and pancreatic lipase levels during a test meal in dogs, *Scand. J. Gastroenterol. 28*, 443−454.
2. Hamilton, J. A., and Small, D. M. (1981) Solubilization and localization of triolein in phosphatidylcholine bilayers: a $^{13}C$ NMR study, *Proc. Natl. Acad. Sci. U.S.A. 78*, 6878−6882.
3. Pieroni, G., and Verger, R. (1979) Hydrolysis of mixed monomolecular films of triglyceride/lecithin by pancreatic lipase, *J. Biol. Chem. 254*, 10090−10094.
4. Borgstrom, B. (1977) The action of bile salts and other detergents on pancreatic lipase and the interaction with colipase, *Biochim. Biophys. Acta 488*, 381−391.
5. Chapus, C., Semeriva, M., Charles, M., and Desnuelle, P. (1978) Adsorption and activation of pancreatic lipase at interfaces, *Adv. Exp. Med. Biol. 101*, 57−68.
6. Gargouri, Y., Pieroni, G., Riviere, C., Sugihara, A., Sarda, L., and Verger, R. (1985) Inhibition of lipases by proteins. A kinetic study with dicaprin monolayers, *J. Biol. Chem. 260*, 2268−2273.

7. Borgstrom, B. (1975) On the interactions between pancreatic lipase and colipase and the substrate, and the importance of bile salts, *J. Lipid Res. 16*, 411−417.
8. Borgstrom, B., Wieloch, T., and Erlanson-Albertsson, C. (1979) Evidence for a pancreatic pro-colipase and its activation by trypsin, *FEBS Lett. 108*, 407−410.
9. Larsson, A., and Erlanson-Albertsson, C. (1991) The effect of pancreatic procolipase and colipase on pancreatic lipase activation, *Biochim. Biophys. Acta 1083*, 283−288.
10. Breg, J. N., Sarda, L., Cozzone, P. J., Rugani, N., Boelens, R., and Kaptein, R. (1995) Solution structure of porcine pancreatic procolipase as determined from 1H homonuclear two-dimensional and three-dimensional NMR, *Eur. J. Biochem. 227*, 663−672.
11. Hermoso, J., Pignol, D., Kerfelec, B., Crenon, I., Chapus, C., and Fontecilla-Camps, J. C. (1996) Lipase activation by nonionic detergents. The crystal structure of the porcine lipase-colipase-tetraethylene glycol monooctyl ether complex, *J. Biol. Chem. 271*, 18007−18016.
12. van Tilbeurgh, H., Egloff, M. P., Martinez, C., Rugani, N., Verger, R., and Cambillau, C. (1993) Interfacial activation of the lipase-procolipase complex by mixed micelles revealed by X-ray crystallography, *Nature 362*, 814−820.
13. Dominguez, C., Sebban-Kreuzer, C., Bornet, O., Kerfelec, B., Chapus, C., and Guerlesquin, F. (2000) Interactions of bile salt micelles and colipase studied through intermolecular nOes, *FEBS Lett. 482*, 109−112.
14. Granon, S. (1986) Spectrofluorimetric study of the bile salt micelle binding site of pig and horse colipases, *Biochim. Biophys. Acta 874*, 54−60.
15. McIntyre, J. C., Hundley, P., and Behnke, W. D. (1987) The role of aromatic side chain residues in micelle binding by pancreatic colipase. Fluorescence studies of the porcine and equine proteins, *Biochem. J. 245*, 821−829.
16. Momsen, W. E., and Brockman, H. L. (1976) Effects of colipase and taurodeoxycholate on the catalytic and physical properties of pancreatic lipase B at an oil water interface, *J. Biol. Chem. 251*, 378−383.
17. Verger, R., Rietsch, J., and Desnuelle, P. (1977) Effects of colipase on hydrolysis of monomolecular films by lipase, *J. Biol. Chem. 252*, 4319−4325.
18. Vandermeers, A., Vandermeers-Piret, M. C., Rathe, J., and Christophe, J. (1975) Effect of colipase on adsorption and activity of rat pancreatic lipase on emulsified tributyrin in the presence of bile salt, *FEBS Lett. 49*, 334−337.
19. Vandermeers, A., Vandermeers-Piret, M. C., Rathe, J., and Christophe, J. (1976) Proceedings: Influence of colipase and biliary salts on the digestion of triglycerides by pancreatic lipase, *Arch. Int. Physiol. Biochim. 84*, 193−195.
20. Momsen, W. E., Momsen, M. M., and Brockman, H. L. (1995) Lipid structural reorganization induced by the pancreatic lipase cofactor, procolipase, *Biochemistry 34*, 7271−7281.
21. Muderhwa, J. M., and Brockman, H. L. (1992) Lateral lipid distribution is a major regulator of lipase activity. Implications for lipid-mediated signal transduction, *J. Biol. Chem. 267*, 24184−24192.
22. Gargouri, Y., Julien, R., Bois, A. G., Verger, R., and Sarda, L. (1983) Studies on the detergent inhibition of pancreatic lipase activity, *J. Lipid Res. 24*, 1336−1342.
23. Castano, S., Desbat, B., Laguerre, M., and Dufourcq, J. (1999) Structure, orientation and affinity for interfaces and lipids of ideally amphipathic lytic LiKj(i = 2j) peptides, *Biochim. Biophys. Acta 1416*, 176−194.
24. Cornut, I., Desbat, B., Turlet, J. M., and Dufourcq, J. (1996) In situ study by polarization modulated Fourier transform infrared spectroscopy of the structure and orientation of lipids and amphipathic peptides at the air-water interface, *Biophys. J. 70*, 305−312.
25. Fullagar, W. K., Aberdeen, K. A., Bucknall, D. G., Kroon, P. A., and Gentle, I. R. (2003) Conformational changes in SP-B as a function of surface pressure, *Biophys. J. 85*, 2624−2632.
26. Stevens, M. M., Allen, S., Sakata, J. K., Davies, M. C., Roberts, C. J., Tendler, S. J., Tirrell, D. A., and Williams, P. M. (2004) pH-dependent behavior of surface-immobilized artificial leucine zipper proteins, *Langmuir 20*, 7747−7752.
27. Fasman, G. D. (1967) *Poly-α-Amino Acids*, New York, NY.
28. Goormaghtigh, E., Cabiaux, V., and Ruysschaert, J. M. (1990) Secondary structure and dosage of soluble and membrane proteins by attenuated total reflection Fourier-transform infrared spectroscopy on hydrated films, *Eur. J. Biochem. 193*, 409−420.
29. Chapus, C., Desnuelle, P., and Foglizzo, E. (1981) Stabilization of the C-terminal part of pig and horse colipase by carboxypeptidase and trypsin inhibitors, *Eur. J. Biochem. 115*, 99−105.
30. Ayvazian, L., Crenon, I., Hermoso, J., Pignol, D., Chapus, C., and Kerfelec, B. (1998) Ion pairing between lipase and colipase plays a critical role in catalysis, *J. Biol. Chem. 273*, 33604−33609.
31. Egloff, M. P., Sarda, L., Verger, R., Cambillau, C., and van Tilbeurgh, H. (1995) Crystallographic study of the structure of colipase and of the interaction with pancreatic lipase, *Protein Sci. 4*, 44−57.
32. Goormaghtigh, E., Cabiaux, V., and Ruysschaert, J. M. (1994) Determination of soluble and membrane protein structure by Fourier transform infrared spectroscopy. III. Secondary structures, *Subcell Biochem. 23*, 405−450.
33. Goormaghtigh, E., Cabiaux, V., and Ruysschaert, J. M. (1994) Determination of soluble and membrane protein structure by Fourier transform infrared spectroscopy. I. Assignments and model compounds, *Subcell Biochem. 23*, 329−362.
34. Blaudez, D., Turlet, J. M., Dufourcq, J., Bard, D., Buffeteau, T., and Desbat, B. (1996) Investigations at the air/water interface using polarization modulation infrared spectroscopy, *J. Chem. Soc. Faraday Trans. 92*, 525−530.
35. Mendelsohn, R., Davies, M. A., Brauner, J. W., Schuster, H. F., and Dluhy, R. A. (1989) Quantitative determination of conformational disorder in the acyl chains of phospholipid bilayers by infrared spectroscopy, *Biochemistry 28*, 8934−8939.
36. Momsen, M. M., Dahim, M., and Brockman, H. L. (1997) Lateral packing of the pancreatic lipase cofactor, colipase, with phosphatidylcholine and substrates, *Biochemistry 36*, 10073−10081.
37. Sugar, I. P., Mizuno, N. K., Momsen, M. M., and Brockman, H. L. (2001) Lipid lateral organization in fluid interfaces controls the rate of colipase association, *Biophys. J. 81*, 3387−3397.
38. Dahim, M., and Brockman, H. (1998) How colipase-fatty acid interactions mediate adsorption of pancreatic lipase to interfaces, *Biochemistry 37*, 8369−8377.
39. Sugar, I. P., Mizuno, N. K., and Brockman, H. L. (2005) Peripheral protein adsorption to lipid-water interfaces: the free area theory, *Biophys. J. 89*, 3997−4005.
40. Nalbone, G., Lairon, D., Lafont, H., Domingo, N., Hauton, J., and Sarda, L. (1974) Behavior of biliary phospholipids in intestinal lumen during fat digestion in rat, *Lipids 9*, 765−770.
41. Sugar, I. P., Mizuno, N. K., Momsen, M. M., Momsen, W. E., and Brockman, H. L. (2003) Regulation of lipases by lipid-lipid interactions: implications for lipid-mediated signaling in cells, *Chem. Phys. Lipids 122*, 53−64.
42. Renard, D., Lefebvre, J., Robert, P., Llamas, G., Dufour, E., and Dufour, E. (1999) Structural investigation of beta-lactoglobulin gelation in ethanol/water solutions, *Int. J. Biol. Macromol. 26*, 35−44.
43. Casal, H. L., Kohler, U., and Mantsch, H. H. (1988) Structural and conformational changes of beta-lactoglobulin B: an infrared spectroscopic study of the effect of pH and temperature, *Biochim. Biophys. Acta 957*, 11−20.
44. Ter-Minassian-Saraga, L., Okamura, E., Umemura, J., and Takenaka, T. (1988) Fourier transform infrared-attenuated total reflection spectroscopy of hydration of dimyristoylphosphatidylcholine multibilayers, *Biochim. Biophys. Acta 946*, 417−423.
45. Wong, P. T., Capes, S. E., and Mantsch, H. H. (1989) Hydrogen bonding between anhydrous cholesterol and phosphatidylcholines: an infrared spectroscopic study, *Biochim. Biophys. Acta 980*, 37−41.
46. Marsh, D. (1996) Lateral pressure in membranes, *Biochim. Biophys. Acta 1286*, 183−223.


BI701831F